Spectrophotometric Study on the Controlling Factor of Molecular Selective Binding of Dyes by Bridged Bis(β-cyclodextrin)s with Diselenobis(benzoyl) Linkers

Yu Liu,* Yun Song, Yong Chen, Zi-Xin Yang, and Fei Ding

Department of Chemistry, State Key Laboratory of Elemento-Organic Chemistry, Nankai University, Tianjin 300071, People's Republic of China

Received: January 23, 2005; In Final Form: April 7, 2005

A series of β-cyclodextrin (β-CD) dimers with 4,4′-diselenobis(benzoyl) linkers, that is, 6,6′-[4,4′-diselenobis(benzoyloxyl)]-bridged bis(β-CD) (**1a**), 6,6′-[4,4′-diselenobis[2-(benzoylamino)ethyleneamino]]-bridged bis(β-CD) (**2a**), and 6,6′-[4,4′-diselenobis[2-(benzoylamino)-3,6-diazaoctylamino]]-bridged bis(β-CD) (**3a**), were synthesized in moderate yields by the reaction of 4,4′-diselenobis(benzoic acid) with β-CD or oligo(ethylenediamino)-6-deoxy-β-CD. Their binding behaviors with some structure-related substrates, such as acridine red (AR), neutral red (NR), rhodamine B (RhB), ammonium 8-anilino-1-naphthalenesulfonate (ANS), and 6-*p*-toluidino-2-naphthalenesulfonic acid (TNS), were investigated in aqueous phosphate buffer solution (pH 7.20) at 298.15 K by means of fluorescence, NMR, as well as circular dichroism spectroscopy and compared with those of their 2,2′-diselenobis(benzoyl)-linked analogues, that is, 6,6′-[2,2′-diselenobis(benzoyloxyl)]-bridged bis(β-CD) (**1b**), 6,6′-[2,3′-diselenobis[2-(benzoylamino)ethyleneamino]]-bridged bis(β-CD) (**2b**), and 6,6′-[2,2′-diselenobis[2-(benzoylamino)-3,6-diazaoctylamino]]-bridged bis(β-CD) (**3b**). The results showed that bis(β-CD)s **1a**−**3a**, whose Se−Se bonds were located at the para position of the carboxyl group, gave stronger binding abilities toward nonlinear guests (RhB and ANS) than their analogues **1b**−**3b**, whose Se−Se bonds were located at the ortho position relative to the carboxyl group. The molecular binding ability and selectivity of model substrates by these ditopic hosts were sufficiently discussed to reveal not only the cooperative contributions of the linker group and CD cavities upon inclusion complexation with dye guest molecules but also the controlling factors for the molecular selective binding.

Introduction

In comparison with natural cyclodextrins (CDs), modified CDs have been known to be able to significantly alter the molecular binding ability and selectivity toward a variety of guests through the simultaneous operation of available weak interactions.[1−7] As a recently developing family of CD derivatives, bridged bis(CD)s can further enhance the molecular binding abilities of monomeric CDs through the cooperative binding of one guest molecule by two hydrophobic CD cavities located in a close vicinity. Consequently, a number of bis(CD)s with considerable structural diversity have been synthesized to investigate their inclusion complexation behaviors that are significantly different from those of their mono-CD counterparts.[8−12] In our preliminary works, we have reported the selective binding behaviors of biquinoline-,[13] bipridine-,[14] oligoethylenediamine-,[15] and organoselenium[16]-bridged bis(β-CD)s with some representative guest molecules in different sizes and shapes. The results showed that these bis(β-CD)s adopted a multiple sandwich binding mode upon inclusion complexation with guest molecules. That is, besides the cooperative association of two CD cavities with two side groups of the guest molecule, the linker group could also provide the additional binding interactions, such as hydrogen bond, electrostatic, and electron transfer interactions, toward the accommodated guest molecule, which would significantly enhance the original binding ability of unmodified CDs, and even change the fluorescence behavior of the guest molecule in some cases. This research advanced our understanding of the intermolecular cooperative complexation behavior and multiple recognition mechanism of bis(β-CD)s. In the present paper, we comparatively investigated the conformations of several bis(β-CD)s linked by 4,4′-diselenobis(benzoyl) and 2,2′-diselenobis(benzoyl) linkers (Chart 1) as well as their inclusion complexation behaviors with some structure-related dye molecules, that is, acridine red (AR), neutral red (NR), rhodamine B (RhB), ammonium 8-anilino-1-naphthalenesulfonate (ANS), and 6-*p*-toluidino-2-naphthalenesulfonic acid (TNS). The obtained results were discussed from the viewpoints of the multiple recognition mechanism and size−fit relationship between host and guest, indicating that the length of the linker group and the size of the pseudocavity formed by the linker group affected the molecular recognition behaviors of bis(β-CD)s to a great degree.

Results and Discussion.

Synthesis. As illustrated in Scheme 1, the bis(β-CD)s 6,6′-[4,4′-diselenobis(benzoyloxyl)]-bridged bis(β-CD) (**1a**), 6,6′-[4,4′-diselenobis[2-(benzoylamino)ethyleneamino]]-bridged bis(β-CD) (**2a**), and 6,6′-[4,4′-diselenobis[2-(benzoylamino)-3,6-diazaoctylamino]]-bridged bis(β-CD) (**3a**) were synthesized in moderate yields by the reaction of 4,4′-diselenobis(benzoic acid) with β-CD or mono[6-oligo(ethylenediamino)-6-deoxyl]-β-CD. Care should be taken to keep the reaction mixture anhydrous and at low temperature during the reactions, particularly in the initial stage, to achieve a smooth and clean reaction without undesirable byproduct(s). The compositions of the obtained bis(β-CD)s were verified by elemental analysis, NMR, as well as FT-IR data, and their conformations were validated by induced

* Corresponding author. E-mail: yuliu@public.tpt.tj.cn.

10.1021/jp0504017 CCC: $30.25
Published on Web 04/30/2005

CHART 1: Molecular Structures of Hosts and Guests

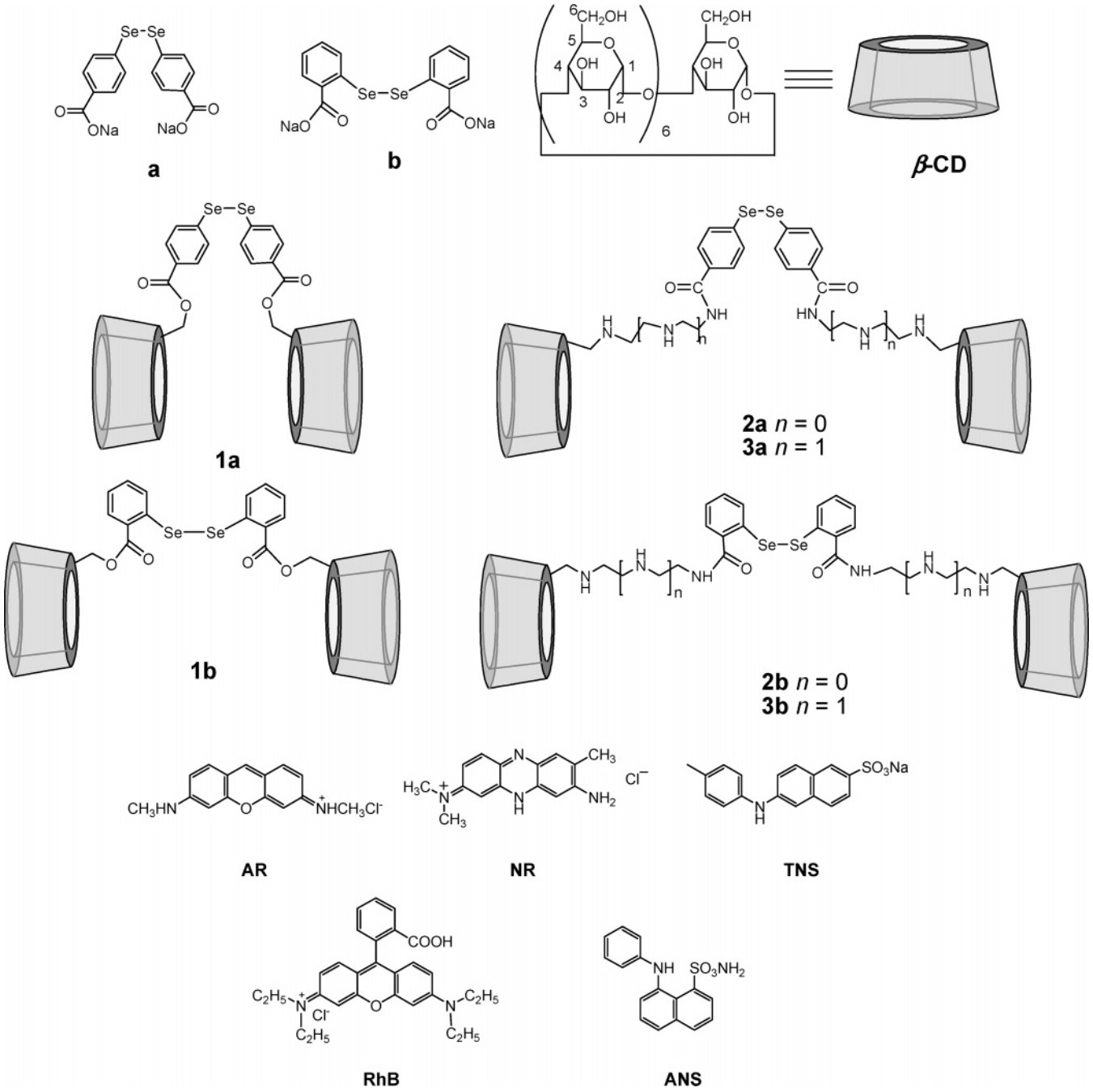

circular dichroism (ICD) and 2D NMR results, as described below.

Conformational Analysis. The initial conformational analysis of CD derivatives is very important to understand their molecular recognition behaviors. It is well-known that the elucidation of crystal structure is one of the most convincing methods of unequivocally illustrating the geometrical conformation of CD derivatives. Unfortunately, our repeated attempts to prepare single crystals of CD dimers that were suitable for X-ray crystallography were unsuccessful. Therefore, we tried to elucidate the conformations of CD dimers through a combinational analysis based on circular dichroism and NMR spectroscopy. Generally, if an achiral guest/moiety is enclosed in or adjacent to a chiral environment, such as a CD cavity, it will give either positive or negative induced circular dichroism (ICD) signals according to its location and orientation related to the CD cavity.[17,18] In the control experiments, the aqueous solutions of **a** and **b** gave neither a circular dichroism signal nor a rotatory signal, which indicated that 4,4′- and 2,2′-diselenobis(benzoyl) groups were achiral chromophores in aqueous solution. To investigate the conformations of β-CD dimers with a chromophoric organoselenium linker, the ICD spectra of **1a**−**3a** were measured at a low concentration of 7×10^{-5} mol·dm^{-3} in aqueous solution. As shown in Figure 1, the substantially different circular dichroism spectra of **1a**−**3a** indicated that different degrees of interactions should exist between the aromatic linker and the chiral CD cavities. The circular dichroism spectrum of **1a** in aqueous solution showed a negative Cotton effect peak at 245 nm ($\Delta\epsilon = -7.09$ M^{-1} cm^{-1}) for the ^1L_a transition and a positive Cotton effect peak at 284 nm ($\Delta\epsilon = 3.72$ M^{-1} cm^{-1}) for the ^1L_b transition of the phenyl group as well as a positive Cotton effect peak at 315 nm ($\Delta\epsilon = 7.52$ M^{-1} cm^{-1}) for the Se−Se transition. As the homologues of **1a**, bis(β-CD)s **2a** and **3a** displayed quite different circular dichro-

SCHEME 1: Synthetic Route of Bis(*β*-CD)s 1a−3a

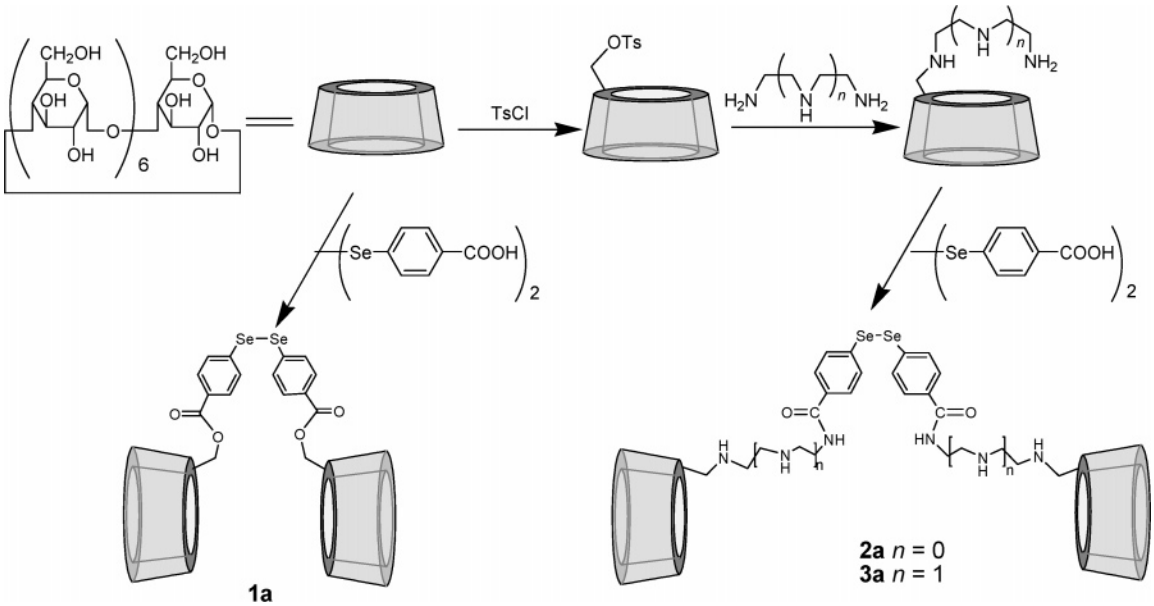

ism patterns from that of **1a**. Bis(*β*-CD) **2a** exhibited two positive Cotton effect peaks for the ^1L_b and ^1L_a transitions of the phenyl group at 297 nm ($\Delta\epsilon = 1.96$ M^{-1} cm^{-1}) and 249 nm ($\Delta\epsilon = 3.92$ M^{-1} cm^{-1}), respectively, as well as a positive Cotton effect peak at 330 nm ($\Delta\epsilon = 1.85$ M^{-1} cm^{-1}) for the Se−Se transition. Bis(*β*-CD) **3a** gave two positive Cotton effect peaks at 285 nm ($\Delta\epsilon = 4.57$ M^{-1} cm^{-1}) and 235 nm ($\Delta\epsilon = 2.62$ M^{-1} cm^{-1}), which might be assigned to the ^1L_b and ^1L_a transitions of the phenyl group, respectively, along with a positive Cotton effect at 307 nm ($\Delta\epsilon = 3.19$ M^{-1} cm^{-1}) for the Se−Se transition. According to the generally accepted empirical rule for CD derivatives,[19−21] the sign of the induced circular dichroism (ICD) signal mainly depended on the orientation of the transition dipole moment of the chromophore with respect to the C_7 axis of the CD. If the guest molecule is located inside the CD cavity or perched on the edge of the CD cavity, its electronic transition parallel to the CD axis gives a positive ICD signal, whereas its perpendicular transition gives a negative signal, but this situation is reversed for a guest located outside the CD cavity. Therefore, we could deduce that the linker group in **2a** or **3a** was located at the exterior of the CD cavity, where both the ^1L_a and ^1L_b transitions of the phenyl chromophore were nearly perpendicular to the CD axis, resulting in the positive Cotton effect peaks. The Se−Se moiety was situated between the two narrow rims of dual CD cavities (Scheme 2); hence,

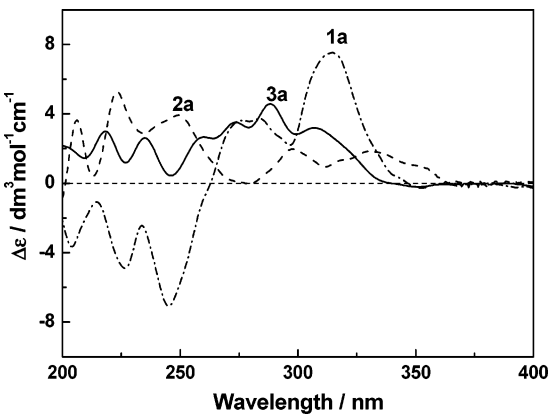

Figure 1. Circular dichroism spectra of bis(*β*-CD)s **1a**−**3a** (7×10^{-5} mol dm^{-3}) in aqueous buffer solution (pH 7.20) at 298.15 K.

SCHEME 2: Schematic Structure of 2a and 3a Deduced from Circular Dichroism Spectra

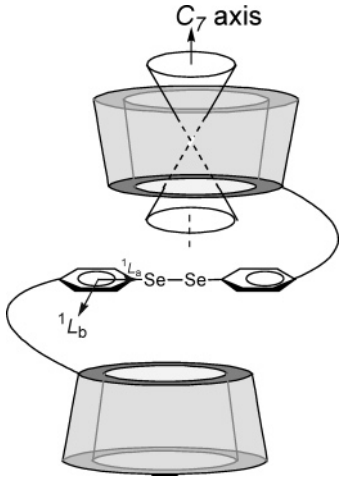

the transition moment of the Se−Se bond was perpendicular to the CD axis, which consequently resulted in the positive Cotton effect. Moreover, the stronger Cotton effect induced by the Se−Se bond in **3a** indicated that the Se−Se bond in **3a** was located closer to the CD rim than that in **2a**. However, for the short-linked bis(*β*-CD) **1a**, the aromatic fragments in the linker group might be either perched on the edge of the CD cavity or self-included in the CD cavity, while the Se−Se transition was nearly perpendicular to the CD axis, which consequently led to the ICD signals as shown in Figure 1. That is to say, the elongation of the linker would be unfavorable to the self-inclusion of aromatic chromophores. This result was consistent with our preliminary report,[16b] where we demonstrated that the benzene ring in 6,6′-[2,2′-diselenobis(benzoyloxyl)]-bridged bis-(*β*-CD) (**1b**) was shallowly self-included in the CD cavity but the benzene ring in 6,6′-[2,3′-diselenobis[2-(benzoylamino)-ethyleneamino]]-bridged bis(*β*-CD) (**2b**) and 6,6′-[2,2′-diselenobis[2-(benzoylamino)-3,6-diazaoctylamino]]-bridged bis(*β*-CD) (**3b**) linked by a longer linker was difficult to be self-included into the CD cavity.

^{1}H NMR investigations further verified the self-inclusion conformation of the linker group in *β*-CD dimer **1a**. In DMSO-d_6, ^{1}H NMR spectroscopy of **1a** only showed two sets of NMR

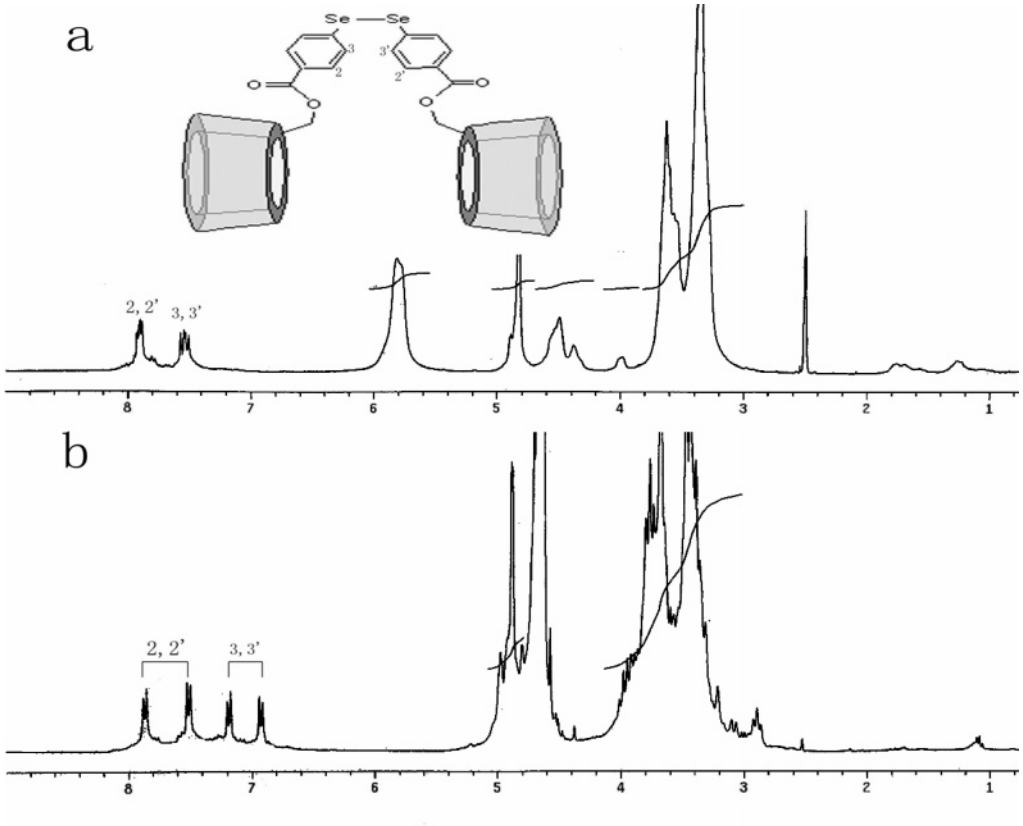

Figure 2. ^{1}H NMR spectra of bis(β-CD) **1a** in (a) DMSO-d_6 and (b) D_2O at 298.15 K.

signals in the aromatic region (δ = 7.4−8.0 ppm) due to the C_2 symmetry of the 4,4′-diselenobis(benzoic carboxylate) unit (Figure 2a). However, four sets of NMR signals were observed in the aromatic region (δ = 6.8−8.0 ppm) of **1a** in D_2O. In addition to the aromatic region, the anomeric (δ = 4.8−5.2 ppm) and nonanomeric (δ = 3.4−3.8 ppm) regions of the spectrum were also affected (Figure 2b). These results apparently indicated that bis(β-CD) **1a** lost its C_2 symmetry in D_2O, which could be explained by the fact that the 4,4′-diselenobis(benzoic carboxylate) linker was partially self-included into the CD cavities because the hydrophobic interactions provided a driving force for this process. When the hydrophobic interactions were absent in DMSO-d_6, the symmetric structure of the 4,4′-diselenobis(benzoic carboxylate) unit was still adopted.[22]

Besides circular dichroism and ^{1}H NMR spectroscopy, two-dimensional NMR spectroscopy is also an efficient method for studying the conformation of CD derivatives, since one can conclude that two protons are closely located in space if an NOE cross-peak is detected between the relevant protons in the NOESY or ROESY spectrum. Therefore, it is possible to determine the orientation of the benzene ring in the cavities of bis(β-CD)s using the assigned NOE correlations, because, if the benzene ring is self-included in the CD's cavity, the NOE correlations between the protons of the benzene ring and the interior protons of the CD should be observed.

The ROESY spectra of **1a** and **1b** in D_2O are shown in Figures 3 and 4, respectively, both displaying strong cross-peaks between the aromatic protons of the linker group and the CD protons. Among these signals, only the cross-peaks with H3, H5, and H6 of the CD could be considered when such results were analyzed because H2 and H4 did not face the inner cavity of the CD and H1 was affected by D_2O. In Figure 3, the cross-peaks A were assigned to the NOE correlations between the 2,2′ and 3,3′ protons of the benzene ring in **1a** and the H3/H5

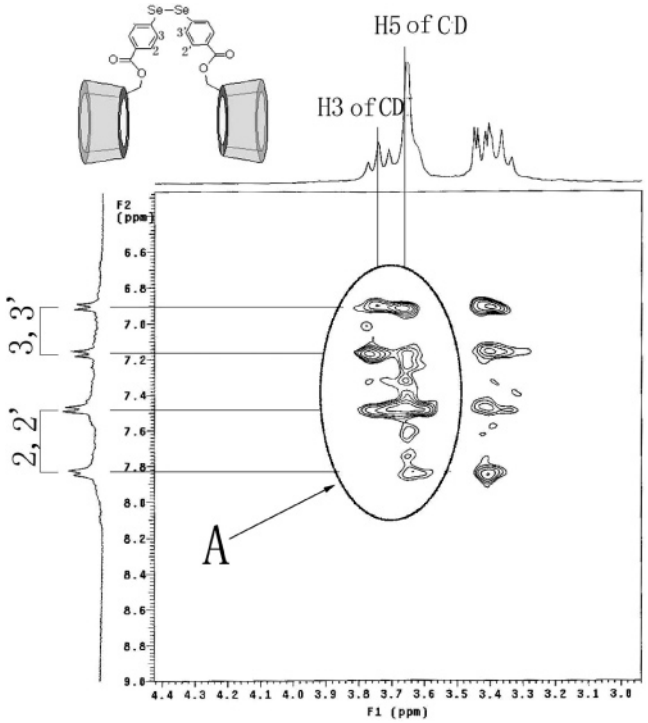

Figure 3. Partial ^{1}H ROESY spectrum (300 MHz) of bis(β-CD) **1a** in D_2O at 298.15 K with a mixing time of 600 ms.

protons of the CD. These results unambiguously indicated that the linker group in bis(β-CD) **1a** was deeply embedded in the CD cavity. In addition, because the H5 protons are located near the narrow side of the CD cavity but the H3 protons near the wide side, the stronger NOE correlations between the 2,2′ and 3,3′ protons of the linker group and the CD's H5 protons indicated that the benzene ring was included in the CD cavity

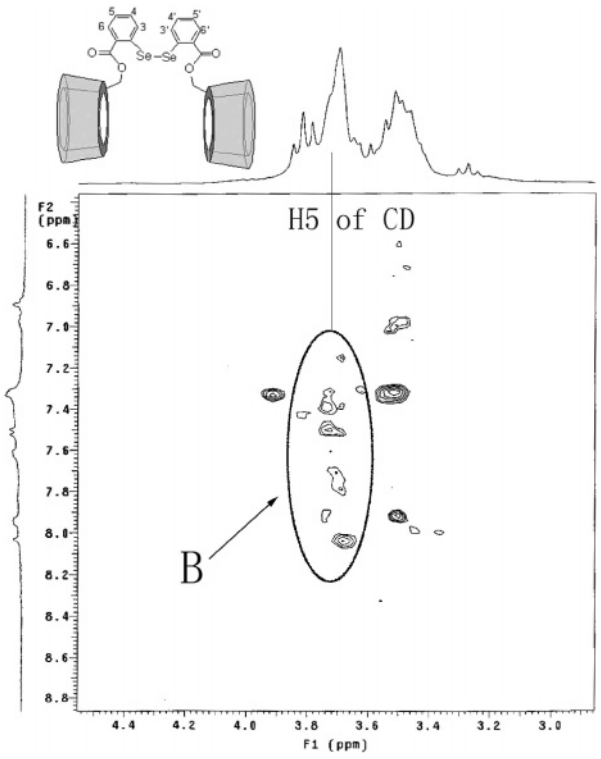

Figure 4. Partial ^{1}H ROESY spectra (300 MHz) of bis(β-CD) **1b** in D_2O at 298.15 K with a mixing time of 600 ms.

from the narrow side. However, for bis(β-CD) **1b** (Figure 4), the aromatic protons of the linker group only gave the obvious NOE correlations with the CD's H5 protons (cross-peaks B), but those correlations with the H3 protons were very weak. This phenomenon indicated that the 2,2′-diselenobis(benzoyl) linker in bis(β-CD) **1b** only shallowly penetrated into the CD cavity from the narrow side. For bis(β-CD)s **2a**, **2b**, **3a**, and **3b** with longer linkers, no NOE correlations could be observed between the linker protons and the interior protons of the CD, indicating that the linker groups in these bis(β-CD)s were not self-included in the CD cavities.

Spectral Titrations. Spectral titrations of bis(β-CD)s with structurally related dye guests were performed at 298.15 K in aqueous phosphate buffer solution (pH 7.20) to quantitatively assess the inclusion complexation behavior of these compounds. In the spectral titration experiments, the concentrations of the dye guests (spectrally active) were kept constant, that is, 0.0034 mM for AR, 0.0034 mM for NR, 0.000 93 mM for RhB, 0.0102 mM for ANS, and 0.0106 mM for TNS, respectively, while the concentrations of the bis(β-CD)s were varied from 0 to 100 times correspondingly in each titration experiment. The spectral changes depended critically on the formation of a new species, that is, a host−guest inclusion complex, showing the spectral enhancement or quenching. As shown in Figure 5, the fluorescence intensity of AR gradually increased with the addition of **1a**. However, in the control experiments, the fluorescence intensities of the dye guests were not appreciably affected by the addition of **a** or **b** under identical conditions. These phenomena indicated that the dye guests must be included in the CD cavities of bis(β-CD)s **1**−**3**, forming the host−guest inclusion complexes.

Assuming 1:1 inclusion complexation stoichiometry between the bis(β-CD) hosts and dye guests, the complex stability constants (K_S) could be calculated by analyzing the sequential changes in fluorescence intensity (ΔI_f) of dye that occurred with changes in host concentration. This analysis was carried out by

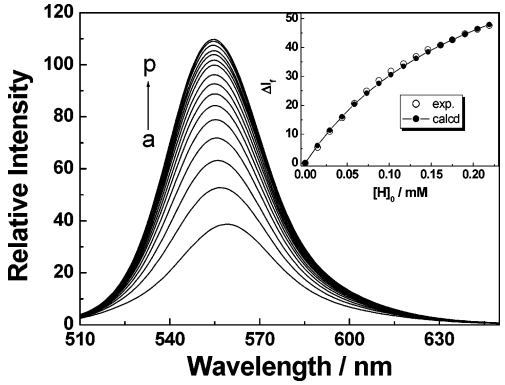

Figure 5. Changes in the fluorescence spectra of AR (3.4×10^{-6} M) upon the addition of bis(β-CD) **2a** (0 and (a−p) 1.46, 2.92, 4.38, 5.85, 7.31, 8.77, 10.2, 11.7, 13.2, 14.6, 16.1, 17.5, 19.1, 20.5, and 21.9×10^{-5} M) in aqueous phosphate buffer solution at 298.15 K and the curve-fitting analysis; $\lambda_{ex} = 490$ nm.

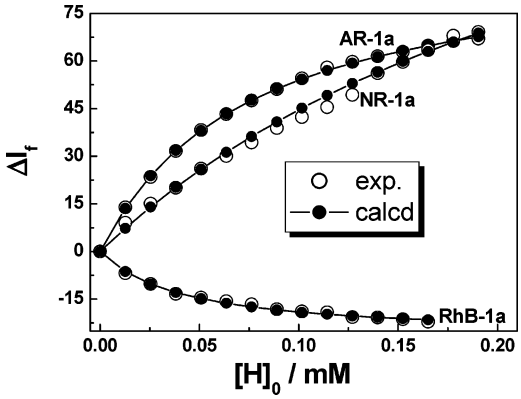

Figure 6. Curve-fitting analyses of the fluorescence titration of AR, NR, and RhB with bridged bis(β-CD) **1a** in aqueous phosphate buffer solution at pH 7.20.

using a nonlinear least-squares curve-fitting method. For each dye guest examined, the plot of ΔI_f as a function of $[H]_0$ gave an excellent fit, verifying the validity of the 1:1 inclusion complexation stoichiometry assumed. The representative curve-fitting analyses of fluorescence titration of organic dyes with host **1a** in an aqueous phosphate buffer solution at pH 7.20 are shown in Figure 6. In the repeated measurements, the K_S values were reproducible within an error of ±5%. The complex stability constants (K_S) obtained for all of the host−guest combinations are listed in Table 1, along with the free energy changes ($-\Delta G°$).

Binding Mode. From Table 1, we can see that all of the bis(β-CD)s gave more or less higher K_S values toward dye guests than native β-CD, which might be attributed to the cooperative binding of two adjacent CD cavities and the potential multiple recognition behavior of such compounds. Generally, the native or mono-modified CDs always include guest molecules into the cavities from the wide openings to minimize the interactions with water and/or decrease the steric hindrance. Superior to the mono-modified CDs, the bridged bis(CD)s, which are connected from not only the primary but also the secondary sides, can significantly enhance the molecular binding ability and selectivity of mono-modified CDs through the cooperative binding of two CD cavities with one guest molecule and the formation of a sandwich-type host−guest complex. Moreover, the spacer can act as an additional binding site for the accommodated guest. To complete the sandwich-type geometry between host and guest, the cooperative binding usually occurs from the smaller openings of the CD cavities[10a,13−16,23] in the case of primary-

TABLE 1: Complex Stability Constants (K_S) and Gibbs Free Energy Changes ($-\Delta G°$) for the Inclusion Complexation of Dye Molecules with β-CD and Bis(β-CD)s in Aqueous Phosphate Buffer Solution (pH 7.20) at 298.15 K Using Fluorescence Titration

host	guest	K_S (M^{-1})	K_S(**X**)/ K_S(β-CD)	log K_S	$-\Delta G°$ (kJ·mol^{-1})	ref
β-CD	AR	2089	≡1	3.3	18.9	ref 14a
	NR	480	≡1	2.7	15.3	ref 16b
	RhB	4240	≡1	3.6	20.7	ref 14a
	ANS	103	≡1	2.0	11.5	ref 16a
	TNS	3670	≡1	3.6	20.4	ref 16a
1a	AR	14 000 ± 200	6.7	4.2	23.7	this work
	NR	3650 ± 50	7.6	3.6	20.3	this work
	RhB	24 700 ± 150	5.8	4.4	25.1	this work
	ANS	3170 ± 60	30.8	3.5	20.0	this work
	TNS	3670 ± 60	1.0	3.6	20.4	this work
2a	AR	4700 ± 100	2.3	3.7	21.0	this work
	NR	1038 ± 30	2.2	3.0	17.2	this work
	RhB	18 900 ± 200	4.5	4.3	24.6	this work
	ANS	5200 ± 100	50.5	3.7	21.2	this work
	TNS	6970 ± 100	1.9	3.8	21.9	this work
3a	AR	5060 ± 80	2.4	3.7	21.1	this work
	NR	1583 ± 50	3.3	3.2	18.3	this work
	RhB	9100 ± 100	2.1	4.0	22.7	this work
	ANS	5540 ± 120	53.8	3.7	21.4	this work
	TNS	11 400 ± 50	3.1	4.1	23.2	this work
1b	AR	3320	1.6	3.5	20.1	ref 16b
	NR	2350	4.9	3.4	19.2	ref 16b
	RhB	11 870	2.8	4.1	23.3	ref 16b
	ANS	1200	11.7	3.1	17.6	ref 16b
	TNS	13 770	3.8	4.1	23.7	ref 16b
2b	AR	2440	1.2	3.4	19.3	ref 16b
	NR	3040	6.3	3.5	19.9	ref 16b
	RhB	5590	1.3	3.8	21.4	ref 16b
	ANS	1370	13.3	3.1	17.9	ref 16b
	TNS	12 900	3.5	4.1	23.5	ref 16b
3b	AR	4320	2.1	3.6	20.8	ref 16b
	NR	1830	3.8	3.3	18.6	ref 16b
	RhB	5060	1.2	3.7	21.1	ref 16b
	ANS	2570	25.0	3.4	19.5	ref 16b
	TNS	10 220	2.8	4.0	22.9	ref 16b

linked bis(CD)s or from the larger openings of the CD cavities[8b,11] in the case of secondary-linked bis(CD)s. To examine the binding mode operative in these diselenobis(benzoyl)-bridged bis(β-CD)s upon cooperative binding with dye guests, we performed the ROESY experiments at 298.15 K in a pD 7.2 phosphate buffer solution. Figure 7 illustrates a typical ROESY spectrum for the inclusion complexation of host **3a** with TNS. As can be easily recognized, this spectrum displays the NOE cross-peaks between TNS protons and the interior protons (H3/H5/H6) of the CD cavity. Through the assignment of these correlations, we could find that the cross-peaks A corresponded to the NOE correlations between the CD's interior protons and the methyl protons of TNS and the cross-peaks B corresponded to the NOE correlations between the protons in the phenyl moiety (Ha and Hb) of TNS and the CD's interior protons, while the cross-peaks C corresponded to the NOE correlations between the naphthalene protons (Hg and Hh) of TNS and the CD's interior protons. Moreover, it could also be observed from the cross-peaks A, B, and C that the corresponding TNS protons (Ha, Hb, Hg, and Hh) all showed stronger correlations with the CD's H5 protons than with the H3 protons. Therefore, we could deduce that the toluene and naphthalene units of TNS were respectively included in two CD cavities from the narrow side to give the sandwich inclusion complex, as illustrated in Figure 9a. In addition, the ROESY spectrum of the **3a**/RhB system (Figure 8) further confirmed the cooperative binding mode of bis(β-CD)s toward guests. As shown in Figure 8, the CD's interior protons gave the NOE

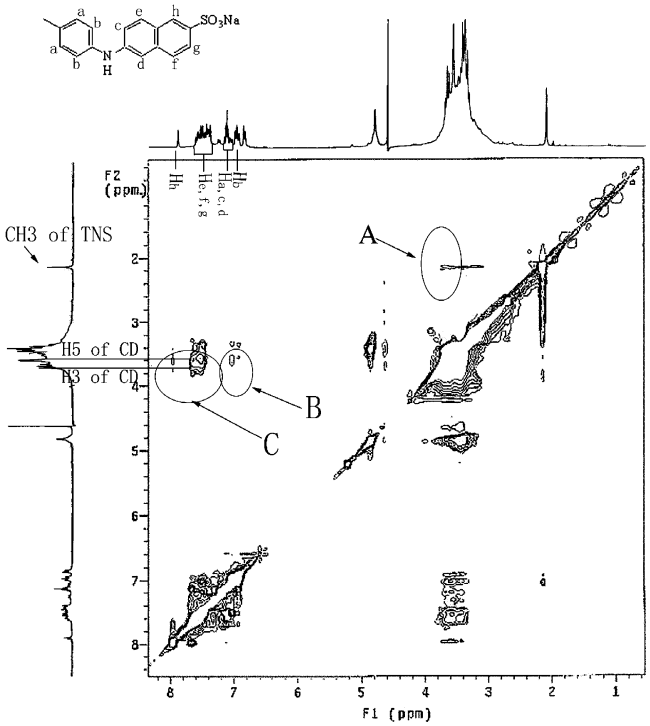

Figure 7. ^{1}H ROESY spectrum (300 MHz) of a mixture of **3a** with TNS ([**3a**] = [TNS] = 5.0×10^{-3} M) in a pD 7.20 buffer solution at 298.15 K with a mixing time of 600 ms.

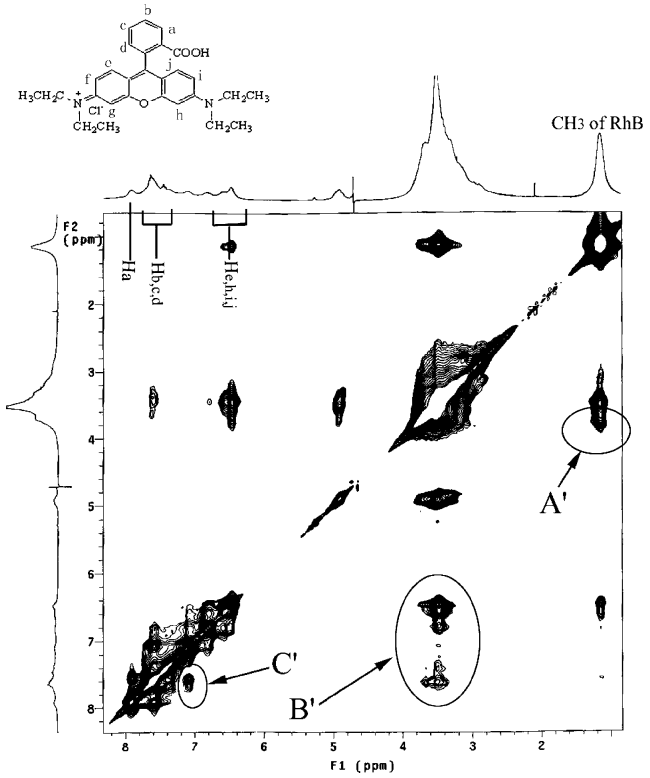

Figure 8. ^{1}H ROESY spectrum (300 MHz) of a mixture of **3a** with RhB ([**3a**] = [RhB] = 5.0×10^{-3} M) in a pD 7.20 buffer solution at 298.15 K with a mixing time of 600 ms.

correlations with not only the methyl protons of diethylamino groups in RhB (cross-peaks A′) but also the aromatic protons of diethylaminophenyl in RhB (cross-peaks B′). Moreover, the cross-peaks C′ clearly demonstrate the close distance between the aromatic protons of the linker group in **3a** and the aromatic protons of the benzoate moiety in RhB. Therefore, we could

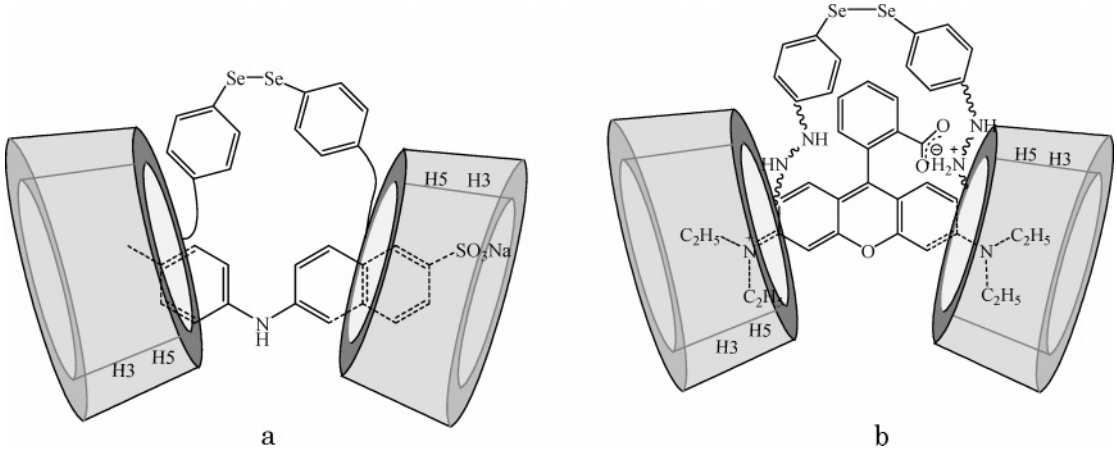

Figure 9. Possible inclusion binding modes of bis(β-CD) with TNS and RhB.

deduce a possible binding mode for the inclusion complexation of bis(β-CD)s with RhB, as illustrated in Figure 9b. That is, two diethylaminophenyl groups of RhB were included in the hydrophobic CD cavities from the narrow side to form a "face-to-face" sandwich inclusion complex, while the benzoate branch of RhB was located in the pseudocavity formed by the linker groups of hosts in part or in whole. Thus, the guest molecule was more efficiently shielded from attack of the bulk water by the cooperative inclusion complexation with CD cavities and the formation of the sandwich host−guest complex. Additionally, under our experimental conditions, the carboxyl group of RhB in aqueous solution was not protonated and should exist as a carboxylate anion and the −NH− fragments in the linker group of bis(β-CD) should be partly protonated. Owing to the electrostatic attraction from the protonated amino groups ($-NH_2^+-$) in the linker, we could also deduce that the negatively charged benzoate component of RhB should penetrate into the pseudocavity of bis(β-CD), which consequently supported the operation of the cooperative multiple binding mode in the complexation of RhB by bis(β-CD)s. From the 2D ROESY experiments, we can unambiguously conclude that the cooperative binding mode from the smaller openings of the CDs was operative in bis(β-CD)s **1**−**3**, as shown in Figure 9.

Molecular Binding Ability and Selectivity. Many reports on the molecular multiple recognition of CD dimers have demonstrated that the functional linker between two CD units plays a crucial role in determining the host−guest binding abilities. The conformation, length, and flexibility of the linker group can control how the CD cavities adjust their orientation and distance to cooperatively bind one guest molecule through the simultaneous operation of several weak forces such as ion−dipole, dipole−dipole, dipole−induced dipole, van der Waals, electrostatic, hydrogen bonding, and hydrophobic interactions according to the size/shape−fit relationship between host and guest. As can be seen in Table 1, the stability constant (K_S) for the complexation of each bis(β-CD) with dye guests decreased in the following order.

1a: RhB > AR > TNS > NR > ANS

2a: RhB > TNS > ANS > AR > NR

3a: TNS > RhB > ANS > AR > NR

1b: TNS > RhB > AR > NR > ANS

2b: TNS > RhB > NR > AR > ANS

3b: TNS > RhB > AR > ANS > NR

In most cases, bis(β-CD)s gave stronger binding affinities toward TNS and RhB than toward other guests. An examination with the Corey−Pauling−Koltun (CPK) molecular model demonstrated that the skeleton lengths of TNS (14.1 Å) and RhB (13.8 Å) were longer than those of AR (10.8 Å), NR (11.1 Å), and ANS (8.1 Å). Therefore, the stronger complexation may be attributed to the strict size−fit between TNS or RhB and bis(β-CD)s, which enabled the long guest to penetrate more deeply into the CD cavity and thus gave the strong van der Waals and hydrophobic interactions between host and guest. Another example for the host−guest size−fit relationship was the binding abilities of bis(β-CD)s toward the guests AR and NR, each of which possessed a heterocycle anthracene moiety. As listed in Table 1, all of the examined hosts except **2b** formed more stable complexes with AR than NR. This result seemed reasonable, since the examination with the CPK molecule model indicated that AR, which possessed two small methylamino substituents, could be well included in the β-CD cavity from the longitudinal direction, while NR could only partly penetrate into the β-CD cavity to form a weaker inclusion complex due to the steric hindrance from the relatively big end groups. In a further investigation, by comparing the enhancement effect of bis(β-CD) for each guest, we can find that the enhancement effect of each guest dye by CD dimers (with the observed enhancement factors shown in the parentheses) was AR (1.2−6.7 times), NR (2.2−7.6 times), RhB (1.2−5.8 times), ANS (11.7−53.8 times), and TNS (1.0−3.8 times), respectively. That is, the shortest guest ANS was able to more fully exploit the cooperative binding of CD dimers rather than the long guests.

It was also interesting to compare the structural features of these bis(β-CD)s with 4,4′-diselenobis(benzoyl) or 2,2′-diselenobis(benzoyl) linkers. Possessing a diselenobis(benzoic carboxylate) unit in the linker group, these bis(β-CD)s shared some structural similarities, but the length of linkers changed in the following order: **3a** > **2a** > **1a**; **3b** > **2b** > **1b**. Another structural difference among these bis(β-CD)s was the location of the Se−Se bond; that is, the Se−Se bond in **1a**−**3a** was located at the para position of the carboxyl group, while in **1b**−**3b** the Se−Se bond was located at the ortho position. These structural similarities and differences among bis(β-CD) analogues may subsequently affect their molecular recognition behavior toward model substrates to some extent. For the linear guests AR, NR, and TNS, even the highest "host selectivities" among bis(β-CD)s **1b**−**3b** were as low as 1.8 (K_{S3b}/K_{S2b}) toward AR, 1.7 (K_{S2b}/K_{S3b}) toward NR, and 1.3 (K_{S1b}/K_{S3b}) toward TNS but were much enhanced to 2.9 (K_{S1a}/K_{S2a}) toward AR, 3.5 (K_{S1a}/K_{S2a}) toward NR, and 3.1 (K_{S3a}/K_{S1a}) toward TNS among bis(β-CD)s **1a**−**3a**. This means the length of the linker group

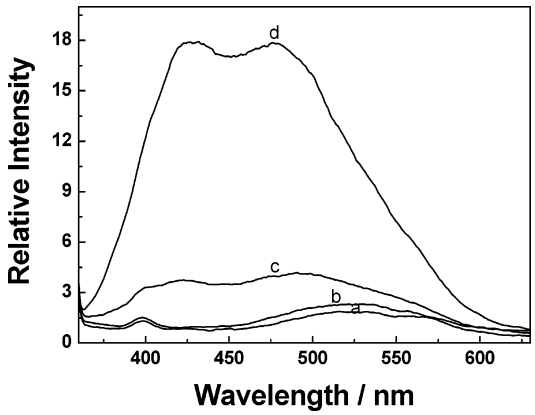

Figure 10. Fluorescence spectra of ANS (1.02×10^{-5} mol dm^{-3}) (a) in the absence and in the presence of (b) β-CD (22.4×10^{-5} mol dm^{-3}), (c) bis(β-CD) **2b** (11.2×10^{-5} mol dm^{-3}), and (d) bis(β-CD) **2a** (11.2×10^{-5} mol dm^{-3}) in phosphate buffer solution (pH 7.2).

gave a more obvious influence on the binding abilities of 4,4′-diselenobis(benzoyl)-bridged bis(β-CD)s **1a**−**3a** than on those of 2,2′-diselenobis(benzoyl)-bridged bis(β-CD)s **1b**−**3b**.

For nonlinear guests, such as T-shaped RhB and L-shaped ANS, each 4,4′-diselenobis(benzoyl)-bridged bis(β-CD) formed more stable complexes than its 2,2′-diselenobis(benzoyl)-bridged analogue. That is, the stability constants (K_S) for the inclusion complexation of RhB and ANS by bis(β-CD)s were in the following order: **1a** > **1b**; **2a** > **2b**; **3a** > **3b**. One possible reason for these host-selectivity sequences may be that the location of the Se−Se bond could affect the size of the pseudocavity formed by the linker group. A calculation based on the CPK model studies demonstrated that the location change of the Se−Se bond from the 2,2′-position to the 4,4-position would enlarge the pseudocavity by ∼13.5 Å^2. That means, in a larger pseudocavity formed by the 4,4′-diselenobis(benzoyl) linker, the branch fragment of a nonlinear guest, such as RhB or ANS, could be appropriately accommodated, and the well-organized pseudocavity could also provide the additional binding interactions with the accommodated branch fragment of the nonlinear guest. These factors jointly resulted in the higher binding affinities of 4,4′-diselenobis(benzoyl)-bridged bis(β-CD)s toward nonlinear guest molecules. However, in the case of 2,2′-diselenobis(benzoyl)-bridged bis(β-CD), the branch fragment of the nonlinear guest could be only partly accommodated in the pseudocavity, owing to the steric hindrance from the Se−Se bond located at the ortho position of the carboxyl group, which would in turn result in the relatively weak combination of bis(β-CD)s **1b**−**3b** with RhB or ANS.

It is also particularly interesting to examine the sensitivity parameter ($\Delta I/I_0$) of the dye guests, where I_0 and I are the fluorescence intensities in the absence and presence of CD hosts, respectively, and ΔI is equal to $I - I_0$. Figure 10 illustrates the typical fluorescence spectra of ANS in the absence and presence of host CDs. The simple reason for choosing ANS as a sensor is that the fluorescence intensity of ANS is sensitive to changes in its environment and is greater in a hydrophobic environment than in a hydrophilic one. As can be seen from Figure 10, ANS displayed a weak fluorescence in the absence of host CDs (trace a). In the presence of β-CD (22 equiv), the sensitivity parameter ($\Delta I/I_0$) of ANS is 23.5% (trace b). However, the addition of 2,2′-diselenobis(benzoyl)-bridged bis(β-CD) **2b** (11 equiv) significantly enhanced the fluorescence intensity of ANS by a factor of 2.2 (trace c), accompanied by an obviously hypsochromic shift (25 nm) of emission peak. More significantly, in the presence of 4,4′-diselenobis(benzoyl)-bridged bis(β-CD) **2a** (11 equiv), ANS showed a much stronger fluorescence up to 9.5 times higher than that of free ANS (trace d), that is, 4.3 times higher than that of the **2b**/ANS system, accompanied by a 40 nm hypsochromic shift of emission peak. This indicated that ANS was most responsive to **2a**. In other cases, the sensitivity parameters of RhB and ANS showed the same orders for all the CD hosts examined, that is, **1a** > **1b** > β-CD; **2a** > **2b** > β-CD; **3a** > **3b** > β-CD, which were the same as the orders of their binding abilities toward these two dye guests. Thus, these phenomena indicated that T-shaped RhB and L-shaped ANS were located in a more hydrophobic environment upon complexation with 4,4′-diselenobis(benzoyl)-bridged bis(β-CD)s than with 2,2′-diselenobis(benzoyl)-bridged bis(β-CD)s. By comparing the structural features of **1a**−**3a** and **1b**−**3b**, we can deduce that the additional environmental hydrophobicity in the case of the **1a**−**3a**/ANS and **1a**−**3a**/RhB systems might come from the well-organized pseudocavity formed by the 4,4′-diselenobis(benzoyl) linker, which more efficiently protected the accommodated ANS and RhB fluorophore from the attack of water molecules and thus resulted in the much enhanced fluorescence. On the other hand, 2,2′-diselenobis(benzoyl)-bridged bis(β-CD)s could only give limited enhancement to the fluorescence of ANS and RhB due to the relatively weak size−fit between the pseudocavity and the branch fragment of ANS and RhB, as described above.

TABLE 2: Complex Stability Constants (K_S) and Gibbs Free Energy Changes ($-\Delta G°$) for the 2a/AR System in the Presence of Alcohols (4 vol %) at 298.15 K

	K_S (M^{-1})	log K_S	$-\Delta G°$ (kJ·mol^{-1})
none	4700 ± 100	3.7	21.0
methanol	1000 ± 60	3.0	17.2
ethanol	3000 ± 60	3.5	19.9
2-propanol	7900 ± 100	3.9	22.3

Solvent Effect. Warner et al. have demonstrated that the addition of a small amount of organic solvents, such as alcohols, could alter the binding abilities of CD hosts toward model substrates in aqueous solution.[24] In this context, we also examine the influence of alcohols on the binding abilities of bis(β-CD)s **1**−**3** toward dye guests. In the fluorescence titration experiments, a small amount (4%, by volume) of methanol, ethanol, or 2-propanol was added to the phosphate buffer solution, and the binding constants of bis(β-CD)s **1**−**3** toward dye guests in the presence and absence of alcohols were quantitatively assessed. The results for a representative **2a**/AR system are listed in Table 2.

From Table 2, we can see that the binding constant of the **2a**−AR complex enhanced from 4700 to 7900 M^{-1} when a small amount of 2-propanol was added but decreased to 1000 or 3000 M^{-1} when methanol or ethanol was added, respectively. For the bis(CD)s linked from the smaller openings of CD cavities, the addition of alcohols could extrude water from the CD cavities and make the cavity more hydrophobic, and thus strengthen the binding of dyes with bis(β-CD)s. On the other hand, some main noncovalent interactions working between host and guest, such as electrostatic and hydrogen bonding interactions, would be weakened to some extent when some water molecules were replaced by alcohols. In the case of adding methanol to the host/guest system, the decrease of electrostatic and hydrogen bonding interactions may be much larger than the increase of hydrophobic interactions, which consequently resulted in the significantly weakened host−guest binding. However, the introduction of a bulky 2-propanol molecule to the host/guest system would extrude a larger amount of water from the CD cavities than small alcohols (e.g., methanol and

ethanol). Therefore, the favorable enhancement of hydrophobic interactions could sufficiently overwhelm the unfavorable decrease of electrostatic and hydrogen bonding interactions, and thus led to the strengthened binding ability between host and guest. Ethanol was located between these two extremes and gave a moderate influence on the binding ability.

Conclusions

The above investigations on the molecular recognition behavior of bis(β-CD)s with 4,4′-diselenobis(benzoyl) and 2,2′-diselenobis(benzoyl) linkers revealed that appropriately controlling the linker length and the location of heteroatoms could give bis(β-CD)s with well-preorganized conformations and consequently result in a strong binding ability and high molecular selectivity toward a model substrate. This concept can be extended more generally to a wide variety of synthetic supramolecular systems and further our understanding of the design and synthesis of new functional supramolecular species.

Experimental Section

General. β-CD of reagent grade was recrystallized twice from H_2O and dried in vacuo for 12 h at 100 °C. *N*,*N*′-Dimethylformamide (DMF) and pyridine were dried over CaH_2 for 2 days and then distilled under reduced pressure prior to use. Bis(β-CD)s **1b**−**3b** were synthesized according to our previous reports.[16] 4,4′-Diselenobis(benzoic acid),[25] mono[6-(2-aminoethyleneamino)-6-deoxy]-β-CD, and mono[6-(5-amino-3-azapentylamino)-6-deoxy]-β-CD[26] were synthesized according to the reported procedures. Elemental analyses were performed on a Perkin-Elmer-2400C instrument. NMR spectra were recorded on a Varian Mercury VX300 instrument. Circular dichroism spectra were recorded in a conventional quartz cell (light path 10 mm) on a JASCO J-715S spectropolarimeter equipped with a PTC-348WI temperature controller to keep the temperature at 298.15 K. Fluorescence spectra were measured in a conventional quartz cell ($10 \times 10 \times 45$ mm^3) at 298.15 K on a JASCO FP-750 spectrometer equipped with a constant-temperature water bath, with excitation and emission slits of 5 nm for all of the fluorescent dyes. The excitation wavelengths for ANS, TNS, NR, AR, and RhB were 350, 366, 493, 490, and 525 nm, respectively. Disodium hydrogen phosphate dodecahydrate (25.79 g) and sodium dihydrogen phosphate dihydrate (4.37 g) were dissolved in 1000 mL of deionized water to make an aqueous NaH_2PO_4/Na_2HPO_4 buffer solution of pH 7.20, which was used in the spectral measurements.

6,6′-[4,4′-Diselenobis(benzoyloxyl)]-Bridged Bis(β-CD) (1a). To a solution of 4,4′-diselenobis(benzoic acid) (0.40 g, 1.0 mmol) in dry DMF (30 mL) containing dicyclohexylcarbodiimide (DCC, 0.7 g, 34 mmol) was added a solution of dry β-CD (2.6 g, 2.29 mmol) in dry pyridine (25 mL). The resultant mixture was stirred for 20 h in an ice bath and for an additional 2 days at room temperature, and then, the precipitate formed was removed by filtration and the filtrate was evaporated under a reduced pressure to dryness. The residue was dissolved in a small amount of hot water, and the aqueous solution was poured into acetone (200 mL) to give a light yellow precipitate. The crude product obtained was dried and purified by column chromatography over Sephadex G-25 with distilled deionized water as eluent to give pure **1a** in 19% yield. ^{1}H NMR (300 MHz, D_2O, TMS): δ 2.8−4.1 (m 84H, C_{2-6}H of CD), 4.8−5.1 (m 14H, C_1H of CD), 6.8−8.0 (m Ar-8H). ^{13}C NMR (300 MHz, D_2O): δ 135.4, 130.9, 129.8, 101.9, 81.1, 73.1, 72.1, 71.8, 60.2. IR (KBr): ν 3340, 2929, 2129, 1715, 1649, 1589, 1542, 1419, 1367, 1288, 1154, 1078, 1030, 945, 846, 758, 706, 578, 531 cm^{-1}. Anal. Calcd for $C_{98}H_{146}O_{72}Se_2 \cdot 9H_2O$: C, 42.10; H, 6.05. Found: C, 42.29; H, 6.22.

6,6′-[4,4′-Diselenobis[2-(benzoylamino)-ethyleneamino]]-Bridged Bis(β-CD) (2a). 2a was prepared in 12% yield from 4,4′-diselenobis(benzoic acid) and mono[6-(2-aminoethyleneamino)-6-deoxy]-β-CD according to similar procedures as those described above. ^{1}H NMR (300 MHz, DMSO-d_6, TMS): δ 2.8−4.0 (m 92H, C_{2-6}H of CD and the methylene protons of $-NHCH_2CH_2NH-$), 4.4−4.6 (m 12H, O_6H of CD), 4.8−5.0 (m 14H, C_1H of CD), 5.6−6.0 (m 28H, $O_{2,3}$H of CD), 7.4−8.0 (m Ar-8H). ^{13}C NMR (300 MHz, D_2O): δ 143.1, 132.8, 128.6, 127.1, 125.0, 117.8, 111.3, 101.9, 81.1, 73.2, 72.1, 71.8, 60.2, 48.3. IR (KBr): ν 3337, 2929, 2129, 1649, 1591, 1541, 1449, 1367, 1329, 1201, 1154, 1078, 1031, 944, 845, 755, 705, 577 cm^{-1}. Anal. Calcd for $C_{102}H_{158}O_{70}N_4Se_2 \cdot 8H_2O$: C, 42.80; H, 6.13; N, 1.96. Found: C, 42.68; H, 6.35; N, 2.28.

6,6′-[4,4′-Diselenobis[2-(benzoylamino)-3,6-diazaoctylamino]]-Bridged Bis(β-CD) (3a). 3a was prepared in 10% yield from 4,4′-diselenobis(benzoic acid) and mono[6-(5-amino-3-azapentylamino)-6-deoxy]-β-CD according to similar procedures as those described above. ^{1}H NMR (300 MHz, DMSO-d_6, TMS): δ 2.8−4.0 (m 100H, C_{2-6}H of CD and the methylene protons of $-NHCH_2CH_2NH-$), 4.4−4.6 (m 12H, O_6H of CD), 4.8−5.0 (m 14H, C_1H of CD), 5.6−6.0 (m 28H, $O_{2,3}$H of CD), 7.4−8.0 (m Ar-8H). ^{13}C NMR (300 MHz, D_2O): δ 136.4, 127.9, 110.0, 102.0, 81.2, 73.5, 72.1, 60.4, 48.6, 46.3. IR (KBr): ν 3331, 2929, 2126, 1647, 1592, 1542, 1455, 1367, 1326, 1153, 1079, 1032, 1000, 944, 844, 756, 705, 577 cm^{-1}. Anal. Calcd for $C_{106}H_{168}O_{70}N_6Se_2 \cdot 15H_2O$: C, 41.41; H, 6.49; N, 2.73. Found: C, 41.40; H, 6.50; N, 2.74.

Acknowledgment. This work was supported by the National Natural Science Foundation of China (Grant Nos. 90306009, 20272028, and 20402008) and the Tianjin Natural Science Foundation (no. 043604411), whom we gratefully acknowledge.

References and Notes

(1) (a) Lebilla, C. B. *Acc. Chem. Res.* **2001**, *34*, 653−661. (b) Monti, S.; Sortino, S. *Chem. Soc. Rev.* **2002**, *31*, 287−300. (c) Easton, C. J.; Lincoln, S. F. *Modified Cyclodextrins Sacffolds and Templates for Supramolecular Chemistry*; Imperial College Press: London, 1999.

(2) (a) Saenger, W.; Jacob, J.; Gessler, K.; Steiner, T.; Hoffmann, D.; Sanbe, H.; Koizumi, K.; Smith, S. M.; Takaha, T. *Chem. Rev.* **1998**, *98*, 1787−1802. (b) Breslow, R.; Dong, S. D. *Chem. Rev.* **1998**, *98*, 1997−2012.

(3) (a) Szejtli, J. *Chem. Rev.* **1998**, *98*, 1743−1754. (b) Szejtli, J.; Osa, T. In *Comprehensive Supramolecular Chemistry*; Lehn, J.-M., Atwood, J. L., Davies, J. E. D., MacNicol, D. D., Vögtle, F., Eds.; Pergamon: Oxford, England, 1996; Vol. 3.

(4) (a) Park, J. W.; Song, H. E.; Lee, S. Y. *J. Phys. Chem. B* **2002**, *106*, 5177−5183. (b) Choi, H. S.; Huh, K. M.; Ooya, T.; Yui, N. *J. Phys. Chem. B* **2004**, *108*, 7646−7650. (c) Kuwabara, T.; Aoyagi, T.; Takamura, M.; Matsushita, A.; Nakamura, A.; Ueno, A. *J. Org. Chem.* **2002**, *67*, 720−725. (d) Liu, Y.; Yang, Y.-W.; Cao, R.; Song, S.-H.; Zhang, H.-Y.; Wang, L.-H. *J. Phys. Chem. B* **2003**, *107*, 14130−14139. (e) Wang, Y.-H.; Zhu, M.-Z.; Ding, X.-Y.; Ye, J.-P.; Liu, L.; Guo, Q.-X. *J. Phys. Chem. B* **2003**, *107*, 14087−14093.

(5) (a) Kitae, T.; Nakayama, T.; Kano, K. *J. Chem. Soc., Perkin Trans. 2* **1998**, 207−212. (b) Rekharsky, M. V.; Inoue, Y. *J. Am. Chem. Soc.* **2002**, *124*, 813−826. (c) Rekharsky, M.; Yamamura, H.; Kawai, M.; Inoue, Y. *J. Am. Chem. Soc.* **2001**, *123*, 5360−5361. (d) Rekharsky, M. V.; Inoue, Y. *J. Am. Chem. Soc.* **2002**, *124*, 12361−12371.

(6) (a) Liu, Y.; Zhao, Y.-L.; Zhang, H.-Y.; Fan, Z.; Wen, G.-D.; Ding, F. *J. Phys. Chem. B* **2004**, *108*, 8836−8843. (b) Park, J. W.; Song, H. E.; Lee, S. Y. *J. Phys. Chem. B* **2002**, *106*, 5177−5183. (c) Park, J. W.; Song, H. E.; Lee, S. Y. *J. Phys. Chem. B* **2002**, *106*, 7186−7192.

(7) (a) Dentuto, P. L.; Catucci, L.; Cosma, P.; Fini, P.; Agostiano, A.; D'Accolti, L.; Trevithick-Sutton, C. C.; Foote, C. S. *J. Phys. Chem. B* **2005**, *109*, 1313−1317. (b) Hause, S. L.; Johanson, E. W.; Green, H. P.; Smith, P. J. *Org. Lett.* **2000**, *2*, 3575−3578.

(8) (a) Breslow, R.; Halfon, S.; Zhang, B. *Tetrahedron* **1995**, *51*, 377−388. (b) Breslow, R.; Yang, Z.; Ching, R.; Trojandt, G.; Odobel, F. *J. Am. Chem. Soc.* **1998**, *120*, 3536−3537. (c) Baugh, S. D. P.; Yang, Z.; Leung, D. K.; Wilson, D. M.; Breslow, R. *J. Am. Chem. Soc.* **2001**, *123*, 12488−12494.

(9) (a) Michels, J. J.; Huskens, J.; Reinhoudt, D. N. *J. Am. Chem. Soc.* **2002**, *124*, 2056−2064. (b) De Jong, M. R.; Engbersen, J. F. J.; Huskens, J.; Reinhoudt, D. N. *Chem.—Eur. J.* **2000**, *6*, 4034−4040. (c) deJong, M. R.; Knegtel, M. A. R.; Grootenhuis, P. D. J.; Huskens, J.; Reinhoudt, D. N. *Angew. Chem., Int. Ed.* **2002**, *41*, 1004−1008.

(10) (a) Breslow, R.; Zhang, B. *J. Am. Chem. Soc.* **1996**, *118*, 8495−8496. (b) Leung, D. K.; Yang, Z. W.; Breslow, R. *Proc. Natl. Acad. Sci. U.S.A.* **2000**, *97*, 5050−5053. (c) Liu, Y.; Zhao, Y.-L.; Chen, Y.; Ding, F.; Chen, G.-S. *Bioconjugate Chem.* **2004**, *15*, 1236−1245. (d) Liu, Y.; Chen, G.-S.; Chen, Y.; Ding, F.; Liu, T.; Zhao, Y.-L. *Bioconjugate Chem.* **2004**, *15*, 300−306. (e) Liu, Y.; Yang, Y.-W.; Song, Y.; Zhang, H.-Y.; Ding, F.; Wada, T.; Inoue, Y. *ChemBioChem* **2004**, *5*, 868−871.

(11) (a) Venema, F.; Rowan, A. E.; Nolte, R. J. M. *J. Am. Chem. Soc.* **1996**, *118*, 257−258. (b) Venema, F.; Nelissen, H. F. M.; Berthault, P.; Birlirakis, N.; Rowan, A. E.; Feiters, M. C.; Nolte, R. J. M. *Chem.—Eur. J.* **1998**, *4*, 2237−2250.

(12) (a) Chiu, S.-H.; Myles, D. C.; Garrell, R. L.; Stoddart, J. F. *J. Org. Chem.* **2000**, *65*, 2792−2796. (b) Yan, J. M.; Breslow, R. *Tetrahedron Lett.* **2000**, *41*, 2059−2062. (c) Benito, J. M.; Garcia, M. G.; Mellet, C. O.; Baussanne, I.; Defaye, J.; Fernàndez, J. M. G. *J. Am. Chem. Soc.* **2004**, *126*, 10355−10363.

(13) Liu, Y.; Song, Y.; Chen, Y.; Li, X.-Q.; Ding, F.; Zhong, R.-Q. *Chem.—Eur. J.* **2004**, *10*, 3685−3696.

(14) (a) Liu, Y.; Li, X.-Q.; Chen, Y.; Guan, X.-D. *J. Phys. Chem. B* **2004**, *108*, 19541−19549. (b) Liu, Y.; Chen, Y.; Li, L.; Zhang, H.-Y.; Liu, S.-X.; Guan, X.-D. *J. Org. Chem.* **2001**, *66*, 8518−8527.

(15) Liu, Y.; You, C.-C.; Li, B. *Chem.—Eur. J.* **2001**, *7*, 1281−1288.

(16) (a) Liu, Y.; Li, L.; Zhang, H.-Y.; Song, Y. *J. Org. Chem.* **2003**, *68*, 527−536. (b) Liu, Y.; Li, B.; You, C.-C.; Wada, T.; Inoue, Y. *J. Org. Chem.* **2001**, *66*, 225−232.

(17) Nakanishi, K.; Berova, N.; Woody, R. W. *Circular Dichroism: Principles and Applications*; VCH: New York, 1994.

(18) Rodger, A.; Nordén, B. *Circular Dichroism and Linear Dichroism*; Oxford University Press: New York, 1997.

(19) Kajtar, M.; Horvath, T. C.; Kuthi, E.; Szejtli, J. *Acta Chim. Acad. Sci. Hung.* **1982**, *110*, 327−355.

(20) Kodaka, M. *J. Am. Chem. Soc.* **1993**, *115*, 3702−3075.

(21) Bright, F. V.; Catena, G. C. *Anal. Chem.* **1989**, *61*, 905−909.

(22) Nelissen, H. F. M.; Feiters, M. C.; Nolte, R. J. M. *J. Org. Chem.* **2002**, *67*, 5901−5906.

(23) (a) Haskard, C. A.; Easton, C. J.; May, B. L.; Lincoln, S. F. *J. Phys. Chem.* **1996**, *100*, 14457-14461. (b) Zhang, B.; Breslow, R. *J. Am. Chem. Soc.* **1997**, *119*, 1676−1681.

(24) (a) Schuette, J. M.; Ndou, T. T.; de la Pela, A. M.; Mukundan, S., Jr.; Warner, I. M. *J. Am. Chem. Soc.* **1993**, *115*, 292−298. (b) Nelson, G.; Patonay, G.; Warner, I. M. *Anal. Chem.* **1988**, *60*, 274−279. (c) Roberts, E. L.; Dey, J.; Warner, I. M. *J. Phys. Chem. A* **1997**, *101*, 5296−5301.

(25) Mlochowski, J.; Kloc, K.; Syper, K.; Inglot, A. D.; Piasecki, E. *Liebigs Ann. Chem.* **1993**, 1239−1244.

(26) Schneider, H.-J.; Xiao, F. *J. Chem. Soc., Perkin Trans. 2* **1992**, 387−391.